

Charge fluctuation between even and odd states of a superconducting island

Yasuhiro Utsumi, Hiroshi Imamura, Masahiko Hayashi, and Hiromichi Ebisawa
Graduate School of Information Sciences, Tohoku University, Sendai 980-8579, Japan
 (November 1, 2018)

We theoretically investigate effects of quantum fluctuation between an even and an odd charge state on the transport properties of a normal-superconducting-normal single-electron tunneling transistor. The charge fluctuation is discussed beyond the orthodox theory. We find that the charging energy renormalization enhances the parity effect: The Coulomb blockade regime for the odd state is reduced and that for the even state is widened. We show that the renormalization factor can be obtained experimentally and that the renormalization effect is weakened by applied bias voltage.

I. INTRODUCTION

Quantum fluctuations play important roles on transport properties of mesoscopic systems at low temperatures. Recently the charge fluctuation in Coulomb islands has attracted much attention. There have been much development in the strong tunneling regime. A theoretical prediction, a renormalization of the conductance and charging energy E_C^{1-5} , has been confirmed experimentally^{6,7}.

When the island is made of superconductor, the “parity effect” plays an important role on transport properties⁸⁻¹². When E_C exceeds the superconducting gap Δ , the parity effect appears in the period of Coulomb oscillation where intervals are either elongated or shortened for even or odd occupancy of electrons respectively. At a resonance, an even and an odd state are degenerate and an unpaired “odd” electron makes dominant contribution to the tunneling current. For $E_C < \Delta$, odd states are no longer stable for every gate voltage and thus $2e$ -periodic Coulomb oscillation appears¹¹.

Therefore, it is an intriguing question to ask how the parity effect with charge fluctuation affect on transport properties. In this paper, we investigate the conduction properties of a superconducting island for $E_C > \Delta$ with a special attention to the charge fluctuation between an even and an odd state. For simplicity we limit ourselves to the discussion at zero temperature limit and neglect the interference effect around tunnel barriers¹². We find that the interval of conductance peaks related to the Coulomb blockade (CB) regime for the odd state is shortened and that related to the even state is widened as a result of the charging energy renormalization. We show that the renormalization factor can be obtained experimentally and that the renormalization effect is weakened by applied bias voltage.

The outline of this paper is as follows. In Sec. II, we introduce the model and derive the generating func-

tional in the path-integral representation. We also propose the approximate generating functional Eq. (2.12). In Sec. III, we derive the current expression by using the functional derivative. In Sec. IV we show numerically evaluated results and have some discussions. Section V summarizes our results.

II. MODEL AND GENERATING FUNCTIONAL

Figure 1(a) shows an equivalent circuit of a normal-superconducting-normal (NSN) transistor. A superconducting island exchanges quasiparticles (QPs) with a left (right) lead via a small tunnel junction characterized by the tunnel matrix element $T_{L(R)}$ and a capacitor $C_{L(R)}$ and is coupled to a gate via a capacitor C_G . In the following discussion, we limit ourselves to the symmetric case, $C_L = C_R$ and $T_L = T_R$. We use the two-state model to describe the strong Coulomb interaction. We assume that there are even (odd) number of electrons in a charge state $|0(1)\rangle$.

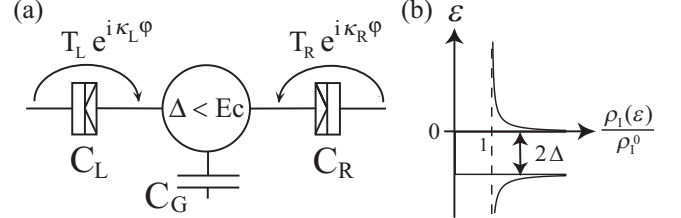


FIG. 1. (a) The equivalent circuit of the NSN transistor. (b) The normalized density of states in the superconducting island.

The total Hamiltonian H is given by the sum of H_0 and a tunneling Hamiltonian H_T , which is adiabatically switched on at remote past and off at distant future. H_0 is defined as

$$H_0 = \sum_{r,k,n} \varepsilon_{rk} a_{rkn}^\dagger a_{rkn} + \Delta_0 \frac{\sigma_z + 1}{2} + E_C (Q_G/e)^2, \quad (2.1)$$

where a_{rkn} is the annihilation operator of a QP in the lead ($r = L, R$) or in the island ($r = I$) with wave vector k and transverse channel n which includes spins. σ is the effective spin-1/2 operator. The second term of Eq. (2.1) describes the energy difference between two charge states. The excitation energy $\Delta_0 = E_C(1 - 2Q_G/e) + \Delta$ is related to a gate charge Q_G . The third term of Eq. (2.1) represents the charging energy for the even state.

The density of states (DOS) for normal metal leads is approximated as constant: $\rho_r(\varepsilon) = \sum_k \delta(\varepsilon - \varepsilon_{rk}) = \rho_r$ ($r = L, R$). Figure 1(b) shows the normalized DOS in the island $\rho_I(\varepsilon)/\rho_I^0$ where ρ_I^0 is DOS for the normal state. We assume that an unpaired electron occupies the lowest energy level above the superconducting gap in the limit of 0 K:

$$\rho_I(\varepsilon) = \frac{\delta(\varepsilon - 0)}{2} + \begin{cases} \frac{\rho_I^0 |\varepsilon + \Delta|}{\sqrt{(\varepsilon + \Delta)^2 - \Delta^2}} & (|\varepsilon + \Delta| > \Delta) \\ 0 & (|\varepsilon + \Delta| \leq \Delta), \end{cases} \quad (2.2)$$

where we consider the condition that the charge and the spin relaxation in the island are enough fast and occupation probabilities for the up- and the down-spin unpaired electron are both 1/2. We expect that the most dominant part of the superconducting correlation effects can be included via the shape of DOS, because any other process than the QP tunneling, such as the Andreev reflection process, requires higher energy $\sim E_C$.

The tunneling Hamiltonian

$$H_T = \sum_{r=L,R} \sum_{k,k',n} T_r e^{i\varphi_r} a_{Ikn}^\dagger a_{rk'n} \sigma_+ + \text{h.c.}, \quad (2.3)$$

describes the electron tunneling across the junctions and simultaneous flip of the effective spin. The phase difference between the lead r and the island is written as $\varphi_r = \kappa_r \varphi$. φ is the phase difference between two leads and is regarded as a source field. $\kappa_{L(R)} = 1/2(-1/2)$ characterizes the voltage drop between the left (right) lead and the island.

The Hamiltonian includes the effective spin-1/2 operator σ and thus the Wick's theorem for fermions or bosons cannot be used. To circumvent this drawback, we employ the drone-fermion representation^{13,14}, which is the map of σ onto two fermion operators c and d as $\sigma_+ = c^\dagger \phi$ and $\sigma_z = 2c^\dagger c - 1$, where $\phi = d^\dagger + d$ is a Majorana fermion operator. In our calculation, we reformulate Ref.¹³ based on the Schwinger-Keldysh approach^{15,16} which enables us to obtain the average current, the current noise and any higher order moments systematically by the functional derivative in terms of the phase difference, *i.e.* a vector potential^{17,18}.

The action can be obtained from the total Hamiltonian H by following the standard procedure¹⁹:

$$\begin{aligned} S[c^*, c, d^*, d, a_{rkn}^*, a_{rkn}] &= \int_C dt \{ c(t)^* (i\hbar \partial_t - \Delta_0) c(t) + i\hbar d(t)^* \partial_t d(t) \\ &+ \sum_{r,k,n} a_{rkn}(t)^* (i\hbar \partial_t - \varepsilon_{rk}) a_{rkn}(t) \\ &+ \sum_{r=L,R} \sum_{k,k',n} T_r e^{i\varphi_r(t)} a_{rkn}(t)^* a_{Ikn}(t) \sigma_+(t) + \text{h.c.} \}, \end{aligned} \quad (2.4)$$

where the derivative and the integration are performed along the closed time-path C consisting of the forward

branch C_+ , the backward branch C_- , and the imaginary time path C_τ ²⁰ (Fig. 2). The degrees of freedom for φ are duplicated, *i.e.*, we can define φ_+ and φ_- on the forward and the backward branch, respectively. a_{rkn} , c and d are Grassmann variables which satisfy the anti-periodic boundary condition. By tracing out QP degrees of freedom⁵ (Appendix. A), we obtain the following effective action for the c - and d -field:

$$\begin{aligned} S[c^*, c, d^*, d] &= \int_C dt \{ c(t)^* (i\hbar \partial_t - \Delta_0) c(t) + i\hbar d(t)^* \partial_t d(t) \} \\ &+ \int_C dt_1 dt_2 \{ \sigma_+(t_1) \alpha(t_1, t_2) \sigma_-(t_2) + O(T_r^4) \}, \end{aligned} \quad (2.5)$$

where trivial constants are omitted. The second integral of Eq. (2.5) describes the tunneling process. $\alpha = \sum_{r=L,R} \alpha_r$ is a particle-hole Green function (GF), written as

$$\alpha_r(t, t') = -i\hbar N_{\text{ch}} T_r^2 \sum_{k,k'} g_{rk}(t, t') g_{Ik'}(t', t) e^{i\kappa_r(\varphi(t) - \varphi(t'))}. \quad (2.6)$$

Here N_{ch} is the number of transverse channels and g_{rk} is a free QP GF in the lead r ($r = L, R$) or in the island ($r = I$). The inverse of g_{rk} is defined as

$$g_{rk}^{-1}(t, t') = (i\hbar \partial_t - \varepsilon_{rk}) \delta(t, t'), \quad (2.7)$$

where δ -function is defined on C and g_{rk} satisfies the anti-periodic boundary condition: $g_{rk}(t, -\infty \in C_+) = -g_{rk}(t, -i\hbar\beta - \infty)$.

In the wide junction limit, $N_{\text{ch}} \rightarrow \infty$, the terms higher than T_r^4 , which describes elastic co-tunneling processes, can be neglected³. The particle-hole GF α describes tunneling and relaxation process related to the lowest order sequential tunneling. However, by tracing out c - or d -field, a number of α are coupled. Therefore, the effective action describes the higher order inelastic co-tunneling processes, too.

Next we trace out drone-fermion fields. Firstly, we trace out the degrees of freedom for c -field. The resulting effective action for d -field includes the many-body interaction, and cannot be solved exactly. Thus we introduce a linear source term $\int_C dt_1 J(t_1) \phi(t_1)$, where J is a Grassmann variable defined on C . By tracing out d -field degrees of freedom, we obtain the generating functional as

$$\begin{aligned} Z &= \exp \left(- \sum_n \frac{(i\hbar)^{2n}}{n} \text{Tr} \left[\left(g_c \frac{\delta}{\delta J} \alpha \frac{\delta}{\delta J} \right)^n \right] \right) \\ &\times \exp \left(- \frac{1}{2i\hbar} \int_C dt_1 dt_2 J(t_1) g_\phi(t_1, t_2) J(t_2) \right) \Big|_{J=0} \\ &\times e^{\text{Tr} \ln [g_c^{-1}]}, \end{aligned} \quad (2.8)$$

where trace is performed over C and products in the trace represent the integration along C . We omit the factor 2

which is the partition function of d -field. Here the c -field and the d -field GFs are defined as

$$g_c^{-1}(t, t') = (i\hbar \partial_t - \Delta_0) \delta(t, t'), \quad (2.9)$$

$$g_\phi^{-1}(t, t') = i\hbar \partial_t \delta(t, t')/2. \quad (2.10)$$

Both GFs satisfy the anti-periodic boundary condition.

The generating functional for connected GF, $W = -i\hbar \ln Z$, is evaluated by performing the perturbation series expansion in powers of α , namely the dimensionless junction conductance $\alpha_0 = \sum_{r=L,R} \alpha_r^0$ where $\alpha_r^0 = N_{\text{ch}} T_r^2 \rho_I^0 \rho_r$. For example, the first order contribution is written as $W^{(1)} = i\hbar \text{Tr} [g_c \Sigma_c]$, where the self-energy $\Sigma_c = \sum_{r=L,R} \Sigma_r$ is defined as

$$\Sigma_r(t, t') = -i\hbar g_\phi(t', t) \alpha_r(t, t'). \quad (2.11)$$

A finite order contribution causes a divergence of the physical quantity, such as the average charge, at the degeneracy point $\Delta_0 = 0$ (Appendix. B). To regularize the divergence, one must take infinite orders into account. The most simple way is to sum up order- n c -field corrections $(g_c \Sigma_c)^n$. This strategy is also adopted by Isawa *et al.* in Ref.¹³, though their formulation is different from ours. The resulting approximate generating functional is expressed as

$$\bar{W} = -i\hbar \text{Tr} [\ln G_c^{-1}], \quad (2.12)$$

where G_c is the full c -field GF whose inverse is defined as

$$G_c^{-1}(t, t') = g_c^{-1}(t, t') - \Sigma_c(t, t'). \quad (2.13)$$

As we show in the next section, the approximate generating functional formally reproduces the result of the resonant tunneling approximation (RTA)^{2,13}.

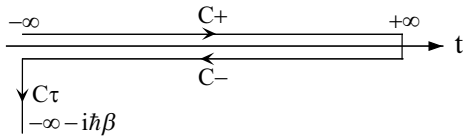


FIG. 2. The closed time-path going from $-\infty$ to ∞ (C_+), going back to $-\infty$ (C_-), connecting the imaginary time path C_τ and closing at $t = -\infty - i\hbar\beta$.

III. AVERAGE CURRENT

The tunneling current is obtained by functional derivative of the generating functional \bar{W} with respect to the phase difference¹⁷ as $I = (e/\hbar) \delta \bar{W} / \delta \varphi_\Delta(t) \big|_{\varphi_\Delta=0} = \sum_{r=L,R} \kappa_r I_r$. The relative coordinate $\varphi_\Delta = \varphi_+ - \varphi_-$ is a fictitious variable and must be 0. The center-of-mass coordinate, $\varphi_c = (\varphi_+ + \varphi_-)/2$, is a physical variable fixed at eVt/\hbar . By regarding φ_r as the formally independent variable, the tunneling current through the junction r , I_r , is expressed as

$$I_r(t) = \frac{e}{\hbar} \frac{\delta \bar{W}}{\delta \varphi_{r\Delta}(t)} \bigg|_{\varphi_\Delta=0} = -e \text{Tr} \left[G_c \frac{\delta \varphi_r}{\delta \varphi_{r\Delta}(t)} \Sigma_r - G_c \Sigma_r \frac{\delta \varphi_r}{\delta \varphi_{r\Delta}(t)} \right] \bigg|_{\varphi_\Delta=0}. \quad (3.1)$$

Here, we pay attention to the fact that only the self-energy depends on the phase difference. Next we project the time defined along C to the real axis. As the tunneling Hamiltonian is turned on and off adiabatically, the particle-hole GF is zero on the imaginary time path C_τ . Thus, Eq. (3.1) is rewritten as,

$$e \text{Tr} \left[\tilde{G}_c \tau^1 \tilde{\Sigma}_r \frac{\delta \tilde{\varphi}_r}{\delta \varphi_{r\Delta}(t)} - \tilde{G}_c \frac{\delta \tilde{\varphi}_r}{\delta \varphi_{r\Delta}(t)} \tilde{\Sigma}_r \tau^1 \right] \bigg|_{\varphi_\Delta=0}, \quad (3.2)$$

where the trace is performed in the 2×2 Keldysh space and products represent the integration along the real axis. τ^s ($s = 0, 1, 2, 3$) is the Pauli matrix in the Keldysh space. Here GF and the phase difference denoted with tilde are the 2×2 matrix for GF and that for the scalar variable in the *physical representation*¹⁶:

$$\tilde{G}_c = \begin{pmatrix} 0 & G_c^A \\ G_c^R & G_c^K \end{pmatrix}, \quad \tilde{\Sigma}_c = \begin{pmatrix} 0 & \Sigma_c^A \\ \Sigma_c^R & \Sigma_c^K \end{pmatrix}, \quad (3.3)$$

$$\tilde{\varphi}_r = Q \begin{pmatrix} \varphi_{r+} & 0 \\ 0 & -\varphi_{r-} \end{pmatrix} Q^\dagger = \varphi_{r+} \tau^1 + \varphi_{r-} \frac{\tau^0}{2}, \quad (3.4)$$

where GFs with superscripts, A , R and K , represent the retarded, the advanced and the Keldysh component, respectively. The practical calculations of these components are shown in Appendix. C. The matrix Q is the Keldysh rotator¹⁶. From Eq. (3.4), we derive the useful relation for the functional derivative technique: $\delta \tilde{\varphi}_r(t') / \delta \varphi_{r\Delta}(t) = \tau^0 \delta(t - t')/2$. By using the property of GF in the physical representation $\tilde{G}(t, t')^\dagger = -\tau^3 \tilde{G}(t', t) \tau^3$, and that of a Pauli matrix $\tau^3 \tau^1 \tau^3 = -\tau^1$, we can see that the second term of Eq. (3.2) is minus the complex conjugate of the first term. By performing the Fourier transformation, Eq. (3.2) becomes as

$$\begin{aligned} & 2e \text{Re} \int dt_1 \text{Tr} \left[\tilde{G}_c(t, t_1) \tau^1 \tilde{\Sigma}_r(t_1, t) \frac{\tau^0}{2} \right] \bigg|_{\varphi_\Delta=0} \\ &= 2e \text{Re} \int \frac{d\varepsilon}{\hbar} \text{Tr} \left[\tilde{G}_c(\varepsilon) \tau^1 \tilde{\Sigma}_r(\varepsilon) \frac{\tau^0}{2} \right] \\ &= e \int \frac{d\varepsilon}{\hbar} \frac{\Sigma_r^K(\varepsilon) G_c^C(\varepsilon)}{2} - (C \leftrightarrow K), \end{aligned} \quad (3.5)$$

where $G_c^C = G_c^R - G_c^A$, *etc.* By using the expressions for the full c -field GF (Eqs. (C16) and (C17)) and those for the self-energy (Eqs. (C14) and (C15)), we obtain the expression for the average current in the limit of 0 K:

$$I = -\frac{G_K}{e} \int_{-eV/2}^{eV/2} d\varepsilon \frac{\alpha_L^K(\varepsilon) \alpha_R^K(\varepsilon)}{\alpha^K(\varepsilon)} 2i \text{Im} G_c^R(\varepsilon), \quad (3.6)$$

where $G_K = e^2/h$ is the conductance quantum and α_r^K is the Keldysh component of the particle-hole GF (Eq. (C9)). The particle-hole GF of the superconducting island in Eq. (3.6) is given by $\alpha_r^K(\varepsilon) = -2\pi i \alpha_r^0 |\rho(\delta\varepsilon^r - \Delta)|$ where $\delta\varepsilon^r = \varepsilon - \kappa_r eV$. The spectral function $\rho(\varepsilon)$ is given by

$$\rho(\varepsilon) = \begin{cases} -\sqrt{\varepsilon^2 - \Delta^2} & (-D < \varepsilon \leq -\Delta) \\ 1/2\rho_1^0 & (|\varepsilon| < \Delta) \\ 1/2\rho_1^0 + \sqrt{\varepsilon^2 - \Delta^2} & (\Delta \leq \varepsilon < D), \end{cases} \quad (3.7)$$

where the high energy cut-off $D (= E_C \gg \Delta)$ is introduced². The imaginary part of the retarded c -field GF $G_c^R(\varepsilon) = 1/(\varepsilon - \Delta_0 - \Sigma_c^R(\varepsilon))$ describes the excitation spectral density of the charge state. The self-energy of c -field is expressed by $\Sigma_c^R(\varepsilon) = \sum_{r=L,R} \alpha_r^0 R(\delta\varepsilon^r - \Delta) - i\gamma(\varepsilon)$, where the function R is written as

$$R(\varepsilon) \sim -2\varepsilon \ln(2D/\Delta) + 2\sqrt{\varepsilon^2 - \Delta^2} \\ \times \text{Re} \left[\tanh^{-1} \left(\frac{D\varepsilon}{\Delta^2 - \sqrt{D^2 - \Delta^2}\sqrt{\varepsilon^2 - \Delta^2}} \right) + h(\varepsilon) \right] \\ - \ln(|(\varepsilon - D)/(\varepsilon + \Delta)|)/\rho_1^0, \quad (3.8)$$

where $h(\varepsilon) = 0$ for $|\varepsilon| < \Delta$ and $h(\varepsilon) = \tanh^{-1}(D/\varepsilon)$ otherwise. The imaginary part of the self-energy $\gamma(\varepsilon) = -\text{Im}[\alpha^K(\varepsilon)]/2$ represents the life-time broadening of the charge state caused by dissipative charge fluctuation. The charge fluctuation described by α^K is suppressed in the low energy range, $0 < \varepsilon < 2\Delta \ll D$, because for the odd state, there are no states for QPs in the range $-2\Delta < \varepsilon < 0$ as shown in Fig. 1(b). The asymmetry in particle-hole GF $\alpha^K(\varepsilon)$ causes the renormalization of the peak position of $\text{Im}G_c^R(\varepsilon)$. It should be noted that the origin of the renormalization is different from that for the normal metal island²⁻⁵ and the double-island²¹ where particle-hole GF is symmetric.

The expression (3.6) is formally equivalent to that obtained within RTA²². The validity of RTA, which is developed for the normal metal island²⁻⁴, is not obvious when the superconducting correlation exists. However, we expect that RTA can be used as a start point of approximation when QP tunneling is the main transport mechanism. The expectation is partly justified by the following two results. First, Eq. (3.6) reproduces the result of the orthodox theory²³ in the limit of small dimensionless junction conductance α_0 . Secondly, in CB regime ($|eV| \ll |\tilde{\Delta}_0|$), Eq. (3.6) is approximately expressed as

$$G_K(2\pi)^2 \alpha_L^0 \alpha_R^0 (2e\Delta V)^{1/2} V / 3\rho_1^0 \tilde{\Delta}_0^2,$$

which is equal to the previous expression obtained by Averin and Nazarov²⁴ in CB regime for the odd state ($|eV| \ll -\tilde{\Delta}_0$) except for the renormalization of the peak position

$$\tilde{\Delta}_0 = \Delta_0 + 2\alpha_0 \Delta \ln(2E_C/\Delta) - \ln(2\rho_1^0 E_C / \pi\alpha_0) / \rho_1^0.$$

As for the CB regime for the even state ($|eV| \ll \tilde{\Delta}_0$), our result does not reproduce the previous result that the inelastic co-tunneling current is zero²⁴. Here we should comment on the limit of the application of RTA. RTA takes account of high-order inelastic co-tunneling processes where at most one particle-hole excitation is created inside the island at a moment². And thus, the simple application of RTA for the even state, where a low-energy particle-hole excitation cannot be created inside the island, causes us to count some undesirable processes. To improve the approximation in CB regime for the even state is outside the scope of this paper.

IV. RESULTS AND DISCUSSIONS

In our numerical calculation, we choose the superconducting gap and DOS as $\Delta/E_C = 10^{-1}$ and $\rho_1^0 E_C = 10^3$, respectively. The variable $\rho_1^0 \Delta = 10^2$ is the same order as that of the Al island whose volume is 10^4 nm^3 . We confirm that our numerical calculation reproduces the spectral sum rule of the full c -field GF $\int d\varepsilon \text{Im}G_c^R(\varepsilon) = -\pi$ within 0.2% accuracy.

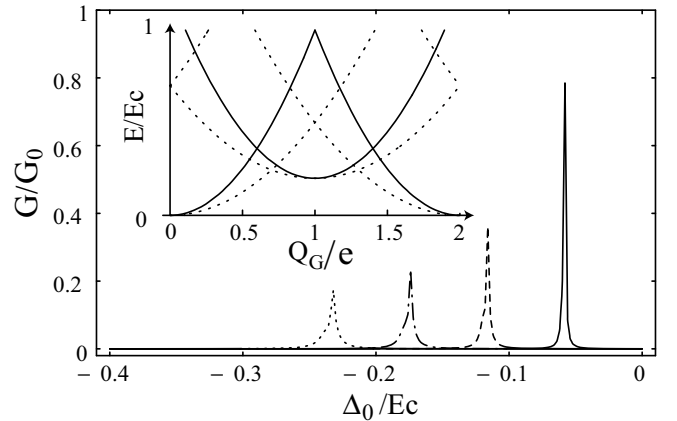


FIG. 3. The excitation energy dependence of differential conductance for $\alpha_0 = 0.1$ (solid line), 0.2 (dashed line), 0.3, (dot-dashed line) and 0.4 (dotted line) at $eV/E_C = 10^{-4}$. Inset: A schematic diagram of the total energy with (dashed lines) and without charge fluctuation (solid lines).

Let us first consider the effect of the charge fluctuation on the conductance G . Using Eq. (3.6), we calculate G as

$$G/G_0 \sim \alpha_0 (1/2\rho_1^0)^2 / \{\tilde{\Delta}_0^2 + (\pi\alpha_0/2\rho_1^0)^2\},$$

where $G_0 = G_K(2\pi)^2 \alpha_L^0 \alpha_R^0 / \alpha_0$. Figure 3 shows the excitation energy dependence of differential conductance at small bias voltage ($eV/E_C = 10^{-4}$) for various α_0 . The width of the conductance peak is approximately given by $\pi\alpha_0/2\rho_1^0$ inversely proportional to the life-time of the unpaired electron. The conductance peak shifts leftward as α_0 increases. The peak position, namely the degeneracy point, is at $\Delta_0 \sim -2\alpha_0 \Delta \ln(2E_C/\Delta)$. At the degeneracy point, the gate charge Q_G/e is approximately

$\Delta/(2zE_C) + 1/2$, where $z = 1/(1 + 2\alpha_0 \ln(2E_C/\Delta))$ is the renormalization factor. The charge fluctuation reduces the charging energy, while it does not affect on the magnitude of the superconducting gap. This result is qualitatively different from that of the normal island, where both of the charging energy and the conductance are renormalized².

The origin of the shift of the degeneracy point can be understood by looking at the schematic diagram of gate charge dependence of the total energy shown in the inset of Fig. 3. The dashed and the solid line indicate the total energy with and without charge fluctuation, respectively. Here we assume that the renormalization factor is independent of Δ_0 . One can see that the curvature of the energy curve with the charge fluctuation is smaller than that without the charge fluctuation since the charging energy is reduced due to the charge fluctuation. Thus the degeneracy points are shifted to reduce CB regime for the odd state.

It should be stressed that the renormalization factor can be determined experimentally. From the Coulomb oscillation, one can obtain the ratio of the superconducting gap to the renormalized charging energy $\Delta/(zE_C) = (Q_G^e - Q_G^o)/(Q_G^e + Q_G^o)$, where $Q_G^{o(e)}$ is the interval corresponding to odd (even) state. Here the “bare” charging energy E_C and the superconducting gap Δ can also be obtained experimentally. For example, one can obtain E_C from the temperature dependence of the conductance peak for the normal state⁶. The superconducting gap Δ can be obtained from the I - V characteristic as discussed below. Therefore, one can estimate the renormalization factor quantitatively by analyzing the experimental results.

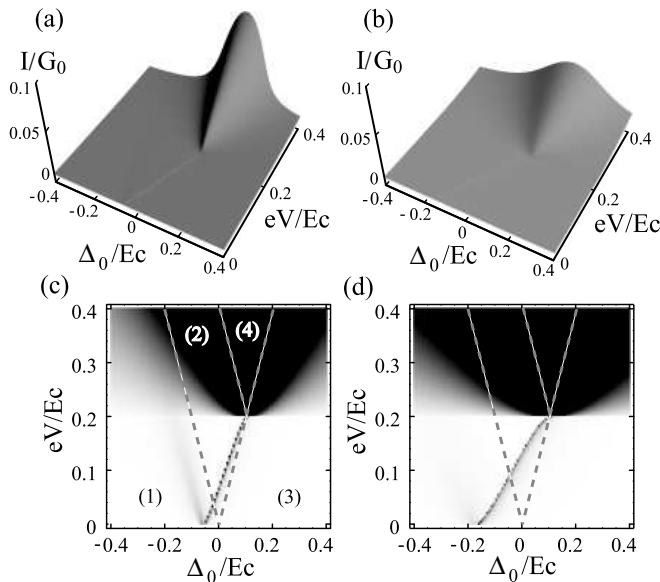


FIG. 4. The excitation energy and the bias voltage dependence of the tunneling current for (a) $\alpha_0 = 0.1$ and (b) 0.3 . The corresponding density plots of differential conductance are shown in panels (c) and (d).

Figures 4(a) and 4(b) show the excitation and bias voltage dependence of the tunneling current for $\alpha_0 = 0.1$ and 0.3 , respectively. The corresponding density plots of differential conductance are shown in Figs. 4(c) and 4(d). Dotted lines indicate boundaries of four regions predicted by the orthodox theory²³: (1) CB regime for the odd state, (2) the unpaired electron tunneling regime, (3) CB regime for the even state, and (4) the QP tunneling regime. The tunneling current shows the plateau in the region (2). As α_0 becomes large (Figs. 4(a) and 4(b)), one can see that the structure of the tunneling current is smeared by the life-time broadening, especially around the QP tunneling regime (4). However, the threshold bias voltage where a QP tunneling channel opens $eV = 2\Delta$ does not depend on α_0 and thus one can obtain Δ experimentally.

The striking feature in Figs. 4(c) and 4(d) is that at the boundary of CB regime for the even state, the conductance peak survives until eV reaches 2Δ . This is because the dissipative charge fluctuation is blocked due to the superconducting gap and only the unpaired electron contributes to the life-time broadening: $\gamma \sim \pi\alpha_0/2\rho_1^0$. On the other hand, at the boundary of CB regime for the odd state, the conductance peak is gradually smeared. This is because the dissipative charge fluctuation increases with increasing bias voltage, and the life-time broadening γ is proportional to the number of QP states: $\gamma \sim \pi\alpha_0\sqrt{\Delta eV}$.

The renormalization effect is expected to be weakened by applied bias voltage because eV gives the low energy cut-off for the renormalization factor⁴. The reduction of the renormalization effect can be deduced by measuring the peak position of the conductance at the boundary of CB regime for the even state (Figs. 4(c) or 4(d)). In the limit of zero bias voltage, the position of the conductance peak deviates from that predict by the orthodox theory(dotted line). As the bias voltage increases, the position of the peak approaches the dotted line and they meet at $eV = 2\Delta$. It means that the renormalization effect is weakened with increasing bias voltage.

V. SUMMARY

In conclusion, we have theoretically investigated the transport properties of NSN transistor showing the parity effect and the quantum fluctuation of charge. We considered the quantum fluctuation between the even and the odd state caused by the inelastic resonant tunneling process. We found that the charge fluctuation causes the renormalization of the charging energy, and that CB regime for the odd state is reduced. The renormalization factor can be obtained experimentally. The renormalization effect is weakened by applied bias voltage. At the boundary of CB regime for the even state, the conductance peak is robust against the charge fluctuation because only one unpaired electron can contribute to the

life-time broadening of the charge state. On the contrary, at the boundary of CB regime for the odd state, the conductance peak is smeared since the dissipative charge fluctuation increases with increasing applied bias voltage.

ACKNOWLEDGMENTS

We would like to thank Y. Isawa, Y. Takane and A. Kanda for valuable discussions. One of us (H. I) is supported by MEXT, Grant-in-Aid for Encouragement of Young Scientists, 13740197, 2001.

APPENDIX A: FUNCTIONAL INTEGRAL ON THE CLOSED TIME-PATH

In this Appendix, we demonstrate the method to calculate the functional integral defined on the closed time path C . For generality, we consider the following action

$$S = \int_C dt \{c(t)^* (i\hbar \partial_t - \varepsilon) c(t) + J(t)^* c(t) + h.c.\}, \quad (\text{A1})$$

where c is a Grassmann variable. A complex variable J is a source field and is zero on C_τ . In order to utilize the time-slicing technique on C^{25} , we introduce the cut-off time $t_0 > 0$ which restricts the range of C_\pm from $-t_0$ to t_0 and we take the limit as $t_0 \rightarrow \infty$ after all calculations. We divide contours C_+ , C_- and C_τ into N pieces, respectively. The discretized time is $t_n = \sum_{i=1,n} \epsilon_i - t_0$ where $\epsilon_n = 2t_0/N$ for $n = 1, \dots, N$, $\epsilon_n = -2t_0/N$ for $n = N+1, \dots, 2N$ and $\epsilon_n = -i\hbar\beta/N$ for $n = 2N+1, \dots, 3N$. The action is written in the discretized form as $\sum_{i,j=1}^{3N} c_i^* A_{ij} c_j + \sum_{i=1}^{3N} \epsilon_i J_i^* c_i + h.c.$, where $A_{ij} = i\hbar \delta_{ij} - (i\hbar + \epsilon_i \varepsilon) \delta'_{i,j+1}$. $\delta'_{i,j+1}$ is the Kronecker's delta $\delta_{i,j+1}$ for $j = 1, \dots, 3N-1$ and $-\delta_{i,1}$ for $j = 3N$. The integration is performed in the same way as the imaginary time path-integral²⁶. By taking the limit as $t_0 \rightarrow \infty$ after taking the continuous limit $N \rightarrow \infty$, we obtain the generating functional as

$$Z = Z_0 \exp \left(\frac{1}{i\hbar} \int_C dt dt' J^*(t) g(t, t') J(t') \right). \quad (\text{A2})$$

Here $Z_0 = \exp \text{Tr} \ln (g^{-1})$ becomes the partition function for fermion, $1 + e^{-\beta\varepsilon}$, because the contribution from C_+ and that from C_- cancel each other and only the contribution from C_τ remains.

Though GF in Eq. (A2) is defined on C , in the practical calculations GF defined on $C_+ + C_-$ is needed. If $t > t'$ with respect to the contour $C_+ + C_-$, $g(t, t')$ is written with the time projected on the real axis as

$$f^+(\varepsilon) \exp(\varepsilon(t - t')/(i\hbar))/(i\hbar), \quad (\text{A3})$$

where $f^+(\varepsilon)$ is defined with the Fermi function $f^-(\varepsilon) = 1/(e^{\beta\varepsilon} + 1)$ as $f^+(\varepsilon) = f^-(\varepsilon) e^{\beta\varepsilon}$. In the opposite case, $t < t'$, $g(t, t')$ is written as

$$-f^-(\varepsilon) \exp(\varepsilon(t - t')/(i\hbar))/(i\hbar). \quad (\text{A4})$$

APPENDIX B: FIRST ORDER PERTURBATION THEORY

In this Appendix, we demonstrate that the lowest order perturbation theory gives the divergent average charge at the degeneracy point within our formulation. For simplicity, we consider the case of the equilibrium state and in the limit of zero temperature. In this case, the imaginary-time formalism²⁶ is convenient for calculations and the grand canonical potential is evaluated perturbatively in the same way as Sec. II. The first order term of the grand canonical potential $\Omega^{(1)}$ becomes the similar form as $W^{(1)}$ and consists of the thermal GF for c -field, d -field and the particle-hole given by $1/(i\omega_l - \Delta_0)$, $2/(i\omega_l)$ ¹⁴ and $\alpha(i\nu_n)$, respectively. Here, ω_l and ν_n are the fermion and the boson Matsubara frequency, respectively.

$$\begin{aligned} \Omega^{(1)} &= \frac{1}{\beta^2} \sum_{l,n} \frac{1}{i\nu_n + i\omega_l - \Delta_0} \frac{2}{i\omega_l} \alpha(i\nu_n) \\ &= \tanh \left(\frac{\Delta_0}{2T} \right) P \int d\varepsilon \frac{-\frac{1}{\pi} \text{Im} [\alpha(\varepsilon + i0)]}{\Delta_0 - \varepsilon} N^-(\varepsilon), \end{aligned}$$

where P denotes the Cauchy's principal value integral and $N^-(\varepsilon) = 1/(e^{\beta\varepsilon} - 1)$ is the Bose distribution function. Here the numerator of the integrand is the spectral function of the particle-hole GF written as $\alpha_0 \rho(\varepsilon - \Delta)$ where ρ is given by Eq. (3.7). The correction of the average charge is evaluated by the derivative of $\Omega^{(1)}$ in terms of the excitation energy². In the limit of zero temperature, it becomes as $\partial\Omega^{(1)}/\partial\Delta_0 \sim \frac{1}{2} \alpha_0 \text{sgn}(\Delta_0) \partial R(\Delta_0 - \Delta)/\partial\Delta_0$ where R is given by Eq. (3.8). As a result, in the CB regime for even state $0 < \Delta_0 \ll E_C$, we can see that the correction diverges as $\sim \alpha_0 \pi \sqrt{\Delta/(2\Delta_0)}/2$, where we omit the contribution from the last term of Eq. (3.8), which is negligible when we consider the life-time effect. For normal state, our formulation reproduces the well known result, the log-divergence²⁷. The divergence for NSN transistor is strong as compared with the log-divergence.

APPENDIX C: GREEN FUNCTIONS

In this Appendix we calculate GFs. Before proceeding to the calculation of each GF, we demonstrate the method to obtain GF by solving the differential equation

$$g^{-1}(t, t') = (i\hbar \partial_t - \varepsilon) \delta(t, t'), \quad (\text{C1})$$

$$g(t, -t_0 \in C_+) = -g(t, -i\hbar\beta - t_0), \quad (\text{C2})$$

as complementary to the method demonstrated in Appendix A²⁸. Here the definition of t_0 is given in Appendix. A. First, we calculate GF defined on C_τ , viz. $t, t' \in C_\tau$. In this case, the δ -function formally satisfies the relation $\int_0^{-i\hbar\beta} dt \delta(t) = 1$. By using the anti-periodic boundary condition Eq. (C2), we can solve Eq. (C1) in the same way as the thermal GF²⁶. From the solution, we can show the following relation as

$$g(-t_0 \in C_\mp, -t_0 \in C_\pm) = \pm f^\pm(\varepsilon)/(i\hbar), \quad (C3)$$

where, we use conditions $g(-t_0 \in C_-, -t_0 \in C_+) = -g(-t_0 \in C_-, -t_0 - i\hbar\beta)$ and $g(-t_0 \in C_+, -t_0 \in C_-) = -g(-t_0 - i\hbar\beta, -t_0 \in C_-)$. Second, we calculate GFs defined on the real axis²⁹. By projecting the time defined on C_\pm , onto the real axis, $g(t, t')$ is projected as $g^{\pm\pm}(t, t')$ for $t, t' \in C_\pm$ and as $g^{\pm\mp}(t, t')$ for $t \in C_\pm$ and $t' \in C_\mp$. It should be careful that the arguments t and t' of GFs with superscripts are the time projected onto the real axis. These four GFs satisfy the following differential equations as

$$(i\hbar\partial_t - \varepsilon) \begin{cases} g^{\pm\pm}(t, t') = \pm\delta(t - t') \\ g^{\pm\mp}(t, t') = 0, \end{cases}$$

where the δ -function is defined on the real axis. These differential equations can be solved by using Eq. (C3) and matching conditions, $g^{s\pm}(t, t_0) = g^{s\mp}(t, t_0)$ and $g^{\pm s}(t_0, t') = g^{\mp s}(t_0, t')$ where $s = +$ or $-$. The resulting GFs are

$$\begin{cases} g^{++}(t, t') = g^{-+}(t, t')\theta(t - t') + g^{+-}(t, t')\theta(t' - t) \\ g^{--}(t, t') = g^{-+}(t, t')\theta(t' - t) + g^{+-}(t, t')\theta(t - t') \\ g^{\mp\pm}(t, t') = \pm f^\pm(\varepsilon) \exp(\varepsilon(t - t')/(i\hbar))/(i\hbar). \end{cases}$$

The results are equivalent to Eqs. (A3) and (A4).

The four GFs are components of 2×2 GF in the *single time representation*¹⁶. It is known that this representation includes the redundancy which can be removed by the Keldysh rotation^{15,16}. After the Keldysh rotation, we obtain 2×2 GF in the physical representation (see Eq. (3.3)). In the following discussions, we summarize the retarded and the Keldysh components of 2×2 GF in the physical representation. The advanced component is obtained by taking the complex conjugate of the retarded component in the energy space.

The differential equation Eq. (2.7) can be solved in the same way as above example:

$$g_{rk}^R(\varepsilon) = 1/(\varepsilon + i\eta - \varepsilon_{rk}), \quad (C4)$$

$$g_{rk}^K(\varepsilon) = -2i\pi \tanh\left(\frac{\varepsilon}{2T}\right) \delta(\varepsilon - \varepsilon_{rk}), \quad (C5)$$

where, η is a positive small value and the δ -function in the energy space is defined as $\delta(\varepsilon) = \frac{1}{\pi} \frac{\eta}{\varepsilon^2 + \eta^2}$.

By using Eqs. (C4) and (C5), we can calculate the retarded and the Keldysh components of particle-hole GF defined by Eq. (2.6). In the following, we fix the relative coordinate of the phase difference as $\varphi_\Delta(t) = 0$, and the

center-of-mass coordinate as $\varphi_c(t) = eVt/\hbar$. The loop diagram can be calculate in the standard way³⁰:

$$\alpha_r^R(\varepsilon) = N_{\text{ch}} T_r^2 \sum_{k, k'} \int \frac{d\varepsilon'}{2i\pi} \times \frac{g_{rk}^R(\delta\varepsilon^r + \varepsilon') g_{lk'}^K(\varepsilon') + g_{rk}^K(\delta\varepsilon^r + \varepsilon') g_{lk'}^A(\varepsilon')}{2} \quad (C6)$$

$$= -i\pi \alpha_r^0 \rho(\delta\varepsilon^r - \Delta), \quad (C7)$$

$$\alpha_r^K(\varepsilon) = N_{\text{ch}} T_r^2 \sum_{k, k'} \int \frac{d\varepsilon'}{2i\pi} \times \frac{g_{rk}^K(\delta\varepsilon^r + \varepsilon') g_{lk'}^K(\varepsilon') - g_{rk}^C(\delta\varepsilon^r + \varepsilon') g_{lk'}^C(\varepsilon')}{2} \quad (C8)$$

$$= -2i\pi \alpha_r^0 \rho(\delta\varepsilon^r - \Delta) \coth\left(\frac{\delta\varepsilon^r}{2T}\right), \quad (C9)$$

where the spectral function $\rho(\varepsilon)$ is defined by Eq. (3.7).

By solving the differential equations (2.9) and (2.10), we obtain GFs for c - and those for d -field:

$$g_\phi^R(\varepsilon) = 2/(\varepsilon + i\eta), \quad (C10)$$

$$g_\phi^K(\varepsilon) = 0, \quad (C11)$$

$$g_c^R(\varepsilon) = 1/(\varepsilon + i\eta - \Delta_0), \quad (C12)$$

$$g_c^K(\varepsilon) = -2i\pi \tanh\left(\frac{\varepsilon}{2T}\right) \delta(\varepsilon - \Delta_0). \quad (C13)$$

The retarded and the Keldysh component of self-energy for c -field Eq. (2.11) are calculated by using Eqs. (C7), (C9), (C10), and (C11):

$$\Sigma_r^R(\varepsilon) = \int \frac{d\varepsilon'}{2\pi} \frac{i \alpha_r^K(\varepsilon')}{\varepsilon + i\eta - \varepsilon'}, \quad (C14)$$

$$\Sigma_r^K(\varepsilon) = \alpha_r^R(\varepsilon) - \alpha_r^A(\varepsilon) = 2\alpha_r^R(\varepsilon), \quad (C15)$$

where we utilize the similar expression as Eqs. (C6) and (C8).

The expressions for full c -field GF is obtained by solving the inverse Dyson equation Eq. (2.13). By projecting the time on C_\pm onto the real axis, and performing the Fourier transformation, we obtain the matrix Dyson equation as $\tilde{G}_c(\varepsilon) = \tilde{g}_c(\varepsilon) - \tilde{g}_c(\varepsilon) \boldsymbol{\tau}^1 \tilde{\Sigma}_c(\varepsilon) \boldsymbol{\tau}^1 \tilde{G}_c(\varepsilon)$. The matrix Dyson equation is solved easily:

$$G_c^R(\varepsilon) = 1/(\varepsilon + i\eta - \Delta_0 - \Sigma_c^R(\varepsilon)), \quad (C16)$$

$$G_c^K(\varepsilon) = G_c^R(\varepsilon) \left\{ \Sigma_c^K(\varepsilon) - 2i\eta \tanh\left(\frac{\varepsilon}{2T}\right) \right\} G_c^A(\varepsilon), \quad (C17)$$

where we use the definition of δ -function in the energy space. Taking the limit $\eta \rightarrow 0$, we obtain the final form for full c -field GF.

¹ G. Falci, G. Schön, and G. T. Zimanyi, Phys. Rev. Lett. **74**, 3257 (1995).

- ² H. Schoeller, and G. Schön, Phys. Rev. B **50**, 18436 (1994).
- ³ J. König, H. Schoeller, G. Schön, and R. Fazio, in *Quantum Dynamics of Submicron Structures*, edited by H. A. Cerdeira *et al.* (Kluwer, Dordrecht, 1995), pp. 221-239.
- ⁴ H. Schoeller, in *Mesoscopic Electron Transport*, edited by L. L. Sohn *et al.* (Kluwer, Dordrecht, 1997), pp. 291-330.
- ⁵ D. S. Golubev, J. König, H. Schoeller, G. Schön, and A. D. Zaikin, Phys. Rev. B **56**, 15782 (1997).
- ⁶ P. Joyez, V. Bouchiat, D. Esteve, C. Urbina, and M. H. Devoret, Phys. Rev. Lett. **79**, 1349 (1997).
- ⁷ D. Chouvaev, L. S. Kuzmin, D. S. Golubev, and A. D. Zaikin, Phys. Rev. B **59**, 10599 (1999).
- ⁸ D. C. Ralph, C. T. Black, J. M. Hergenrother, J. G. Lu and M. Tinkham, in the same book as Ref.⁴, pp. 447-467, and references therein.
- ⁹ R. Fazio and G. Schön, in the same book as Ref.⁴, pp. 407-446.
- ¹⁰ Y. Utsumi, M. Hayashi and H. Ebisawa, J. Phys. Soc. Jpn. **69**, 2739 (2000).
- ¹¹ F. W. J. Hekking, L. I. Glazman, K. A. Matveev and R. I. Shekhter, Phys. Rev. Lett. **70**, 4138 (1993).
- ¹² F. W. J. Hekking and Yu. V. Nazarov, Phys. Rev. Lett. **71**, 1625 (1993).
- ¹³ Y. Isawa and H. Horii, J. Phys. Soc. Jpn. **69**, 655 (2000).
- ¹⁴ H. J. Spencer, Phys. Rev. **167**, 434 (1968).
- ¹⁵ L. V. Keldysh, Sov. Phys. JETP **20**, 1018 (1965).
- ¹⁶ K.-C. Chou, Z.-B. Su, B.-L. Hao and L. Yu, Phys. Rep. **118**, 1 (1985).
- ¹⁷ A. Kamenev and A. Andreev, Phys. Rev. B **60**, 2218 (1999).
- ¹⁸ D. B. Gutman and Y. Gefen, Phys. Rev. B **64**, 205317 (2001).
- ¹⁹ V. S. Babichenko and A. N. Kozlov, Solid State Commun. **59**, 39, (1986).
- ²⁰ M. N. Kiselev and R. Oppermann, Phys. Rev. Lett. **85**, 5631, (2000).
- ²¹ T. Pohjola, J. König, H. Schoeller and G. Schön, Phys. Rev. B **59**, 7579 (1999).
- ²² Exactly speaking, our result is formally equivalent to that of Ref.², however not equivalent to the result of Ref.¹³. In Ref.¹³, an excess sequential tunneling process is proposed, in addition to the resonant tunneling process².
- ²³ G. Schön, J. Siewert and A. D. Zaikin, Physica B **203**, 340 (1994).
- ²⁴ D. V. Averin, and Yu. V. Nazarov, Phys. Rev. Lett. **69**, 1993 (1992).
- ²⁵ K. Okumura and Y. Tanimura, Phys. Rev. E **53**, 214 (1996).
- ²⁶ J. W. Negele, and H. Orland, *Quantum Many-Particle Systems* (Addison-Wesley Publishing Company, Redwood City, California, 1988).
- ²⁷ G. Schön, in *Quantum Transport and Dissipation*, edited by T. Dittrich *et al.* (Wiley-VCH, Weinheim, 1998), pp. 149-212.
- ²⁸ Though this is the basic knowledge for Keldysh formalism, we dare to explain the method to solve Eq. (C1). Because there is no reasonable text book which explains the method to solve the differential equation defined not on the Keldysh contour $C_+ + C_-$ but on the contour C .
- ²⁹ Once the boundary condition at $t = -t_0$ is determined as Eq. (C3), the following process becomes equal in the case of the Keldysh contour $C_+ + C_-$.
- ³⁰ The method to calculate the loop diagram is presented in the review [J. Rammer, and H. Smith, Rev. Mod. Phys. **58**, 323 (1986)]. For example, we calculate the retarded and the Keldysh components of the loop diagram $\Pi(t, t') = g_1(t, t') g_2(t', t)$. $\Pi^R(t, t')$ and $\Pi^K(t, t')$ can be obtained by calculating the trace of 2×2 matrices $\text{Tr}[\tau^0 \tilde{g}_1(t, t') \tau^1 \tilde{g}_2(t', t)]/2$ and $\text{Tr}[\tau^0 \tilde{g}_1(t, t') \tau^0 \tilde{g}_2(t', t)]/2$, respectively. By using the relation $g_1^{R(A)}(t, t') g_2^{R(A)}(t', t) = 0$, we obtain the final expressions: $\Pi^R(t, t') = \{g_1^R(t, t') g_2^K(t', t) + g_1^K(t, t') g_2^A(t', t)\}/2$ and $\Pi^K(t, t') = \{g_1^K(t, t') g_2^K(t', t) - g_1^C(t, t') g_2^C(t', t)\}/2$.